



AIAA 2002-8039
Chemical and Flowfield Modeling for
Enhanced Analysis of Contamination
Experiments

Matthew Braunstein
Spectral Sciences, Inc.
99 South Bedford Street, Suite 7
BURLINGTON, MA 01803

40th Aerospace Sciences Meeting
14-17 January 2002
Reno, Nevada

For permission to copy or to republish, contact the copyright owner named on the first page.
For AIAA-held copyright, write to AIAA Permissions Department,
1801 Alexander Bell Drive, Suite 500, Reston, VA, 20191-4344.

CHEMICAL AND FLOWFIELD MODELING FOR ENHANCED ANALYSIS OF CONTAMINATION EXPERIMENTS*

Matthew Braunstein
Spectral Sciences, Inc.
99 S. Bedford Street, # 7
Burlington, MA 01803

Abstract

This paper describes the application of a new Direct Simulation Monte Carlo (DSMC) code, the Molecular Beam Simulator (MBS), which is designed to analyze laboratory scale molecular beam-surface (and crossed-beam) experiments. The MBS is primarily intended to model experiments associated with spacecraft contamination effects, but it can also be used to simulate a variety of surface chemistry and reactive flow measurements. The MBS code is fully three-dimensional, includes a wide-range of chemical processes, and can model one or multiple pulsed (non-steady) sources. As an example application of the MBS code, a fast, pulsed, oxygen atom-surface experiment which examines the chemistry behind erosion of graphite by oxygen atoms is analyzed. Unsteady DSMC simulations show that experimental observations of excited molecular states after the pulse has hit the surface are consistent with two distinct chemical mechanisms: a direct one where the excited molecules are formed on the surface, and a two-step mechanism where ground state molecules formed on the surface are collisionally excited after they leave the surface by trailing oxygen atoms in the pulse. Further DSMC calculations suggest experiments which can distinguish between these mechanisms.

Introduction

Since the development of the Direct Simulation Monte Carlo (DSMC) method in the 1970's by G. A. Bird,¹ the DSMC approach has proven extremely

useful in modeling rarefied chemically reacting flows.² Because the simulations are done on a molecule-by-molecule basis, a great deal of physical and chemical detail can be included. At the same time, the DSMC approach can compute macroscopic observables, like densities and temperatures, which can be directly compared with measured data. This is done by averaging over a large number of simulated molecular events in a Monte Carlo fashion. The original DSMC method has been adapted to particular conditions for a diverse set of applications. The Molecular Beam Simulator (MBS) code is a refinement of a DSMC code for exhaust plume-atmosphere interactions,⁴ based on Bird's original formulation. The MBS code has been designed to investigate laboratory scale molecular crossed beam and beam-surface contamination measurements.

One of the main uses of the MBS code is to enable a more accurate extraction of fundamental chemical rates from molecular beam experiments. This was shown in an earlier application of the MBS to analyze a molecular beam experiment to measure the excitation cross section of CO by O at high velocity.³ It was shown that multiple-collision effects not considered in the original experimental analysis could have a dramatic effect on the final derived values of the O + CO gas-phase excitation cross section, making the measurements consistent with theoretically derived values. The MBS can also be used to investigate different hypotheses for chemical mechanisms. This can be done by iteratively varying the DSMC input reaction cross sections and/or allowed chemical steps and matching the output with

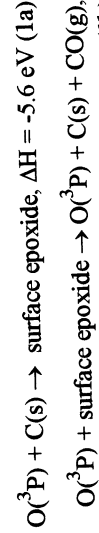
* Copyright © 2002 Spectral Sciences, Inc. Published by the American Institute of Aeronautics and Astronautics, Inc. with permission.

macroscopic experimental observables. The purpose of the present paper is to illustrate such an application to a gas-surface experiment involving fast, pulsed O atoms impacting graphite and producing ground and excited CO,⁵ an important system for understanding erosion of spacecraft materials. It will be shown that the experimental observations are consistent with two distinct chemical mechanisms: a direct one where the excited molecules are formed on the surface, and a two-step mechanism where ground state molecules formed on the surface are collisionally excited after they leave the surface by trailing O atoms in the pulse.

The paper proceeds as follows. We first describe the experiment and the details of the DSMC modeling parameters. We then discuss the results, including detailed spatial and time resolved snapshots of reactants and products, and compare these to the available experimental observations. We then suggest experimental conditions which would distinguish between the two mechanisms. Finally we summarize our results.

Description of the Measurement and DSMC Modeling Parameters

This experiment is fully described in Ref. 5. The purpose was to investigate infrared emission from 1.5 to 6 μm from surfaces due to impacts of atomic oxygen at velocities close to those obtained in low Earth orbit, ~8 km/s (~5 eV impact energy). Erosion of space craft materials due to atomic oxygen has been well studied, and has important implications in materials design.^{6,7} For Kapton, a hydrocarbon 'model' material for such investigations, the nominal erosion yield is ~3e24 $\text{cm}^3/\text{atomic impact}$, which translates to a mass loss of ~2.5 amu's for each oxygen striking the surface.^{6,7} The exact mechanism for surface erosion, however, is not known. For graphite, Cohen⁸ estimates a probability of ~0.2 for loss of a carbon due to an oxygen surface impact, which is consistent with results for Kapton and other hydrocarbons. CO is the main product for atomic oxygen on graphite, but the basic mechanism of its formation remains speculative. Cohen, for example, modeled the formation of CO, in two steps:⁸



The formation of the surface epoxide proceeds through a singlet-triplet curve crossing and

determines the overall erosion probability. The second endothermic step is consistent with an apparent energy threshold for surface erosion. Observations of surface emission, as in Ref. 5, are important in piecing together the basic mechanism for such surface chemistry.

The main elements of the experimental set-up are shown in Figure 1. A pulse of atomic oxygen traveling at 10 km/s is produced by irradiating O₂ with a high power CO₂ laser. (Besides atomic oxygen, O₂ ions, and electronically excited atomic oxygen are produced in the beam in smaller quantities.) Roughly 4e17 O atoms are produced per shot and travel 85 cm to impact surface samples which are 8 by 10 inches. Two kinds of optical set-ups at right angles to the beam for observing emission after each shot were used. One had a wide field of view and captured all the emission and one had narrow fields of view centered at 4 cm and 17 cm in front of the surface for velocity measurements. Band passes separated into 9 bands of about ~0.5 μm wide from 1.5 to 5.5 μm were used. From the measurements, observed radiation levels are related to reaction efficiencies for producing molecular excited states. From spectral fitting, excited CO, CO₂, and OH are observed for surface samples of graphite and polyethylene. We restrict our analysis of the experimental data to O + graphite.

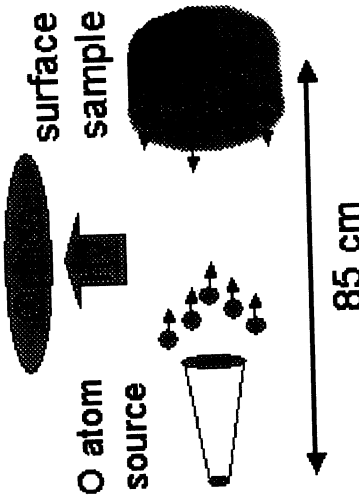


Figure 1. Main elements of gas-surface experiment, after Ref. 5.

We now describe the modeling assumptions for the DSMC calculations. Because we did not have a complete description of the source flow parameters, we followed the set-up of Ref. 9 which has a full description and is quite similar to the present surface experiment. A simple Brook source flow model¹⁰

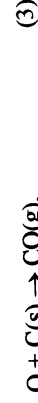
was used for the oxygen atom pulse. Here the number density of atomic oxygen, n_e , is

$$n_e = (B/r^2) \exp(-\lambda^2 (1-\cos(\theta)), \quad (2)$$

where B was $2.24e17$ molecules/cm, $\lambda^2 = 28.5$, r is the radial distance from the source and θ is the angle measured from the maximum flux axis which is directed toward the center of the surface sample. This gives a number density of $\sim 3e13$ atoms/cm³ at 85 cm (at the surface), and a width at half maximum of about 40 cm. Also following reference 9, we assume a pulse length of 7.e-5 seconds. This yields a flux of about $1.e15/cm^2/pulse$ at the surface which is about 10 times larger than that reported in Ref. 5. We discuss these implications later, but mainly this re-normalizes some of the unknown constants of the experimental set-up. The surface was modeled as a thin disk with a radius of 25 cm which extended somewhat farther than the half maximum point of the beam. The scaled Cartesian computational grid consisted of 30 cells in each dimension with lengths of ~ 1 cm near the origin centered on the middle of the surface to ~ 7 cm near the edge of the computational volume which was $100x100x100$ cm³ in total. Vacuum boundary conditions are assumed. The simulation time step was $2.17e-7$ seconds. A nominal collision time near the surface is $1/(\rho\sigma) = 1/(3e13cm^3 * 1.e-15cm^2 * 1.e6cm/s) = 3.33e-5$ seconds, and the nominal mean free path is $1/(\rho\sigma) = 25$ cm.

Unsteady calculations were performed starting from the initiation of the pulse at time zero and extending to $5.e-4$ seconds with sampling done at even increments every $\sim 4.2e-5$ seconds. About 2000 samplings were done for each complete DSMC run. An α value of 0.25 was used for all gas phase collisions.

We allowed to two types scenarios, one where CO excited states are formed on the surface and one where the excited states are formed in the gas phase. For the case of surface excited state formation we assumed that the following reactions could occur for each atomic oxygen impact:



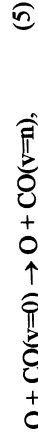
where the CO could be formed in the ground vibrational state or an excited vibrational state up to $v=9$. Each CO state is treated as a separate species. The probabilities to form each vibrational state are: 0.08, 0.0057, 0.0043, 0.0030, 0.0023, 0.0016, 0.0012, 0.00036, 0.00064, 0.00040, for the CO $v=0-9$

vibrational states, respectively. These probabilities reflect the experimentally observed 10,000 K vibrational temperature (determined from spectral fits of the data) and are normalized to a total probability of 0.1 for producing CO. An activation energy of zero was assumed. CO molecules leave the surface with a distribution of velocities which is a weighted fraction of the specular atomic oxygen and a cosine distribution with a magnitude based on the surface temperature, here assumed to be 220 K. The specular fraction for all CO states was chosen as 0.113 giving a velocity of ~ 1.3 km/s which is the experimentally observed³ velocity of excited CO leaving the surface. Single photon decay of the vibrationally excited gas phase CO is also modeled in all the DSMC simulations.



with the known decay rates. For the $v=1$ to $v=0$ transition, for example, the decay time is 0.033 seconds, which is large compared to the total simulation time.

For the case where excited CO is formed in the gas phase, *only* $CO(v=0)$ is allowed to be formed from oxygen atom surface impacts with the same probability and specular fraction as the case described above. However, an additional set of gas phase reactions are allowed:



where $n=1-9$. The cross sections for these reactions follow from those calculated in Ref. 11. A Larsen-Borgnakke model¹ is used to keep track of the internal energy of each CO vibrational species produced. The variable-hard-sphere (VHS) model is used for gas phase collisions, so the direction of post-collision molecules is assumed to be isotropic. Single photon decay for vibrationally excited CO is also included as above. In all cases, atomic oxygen which did not react on the surface is modeled as being fully accommodated with a velocity magnitude reflective of the assumed surface temperature and a cosine angular distribution.

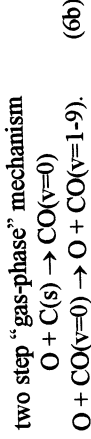
Results of DSMC Modeling

A basic experimental assumption we wish to test with DSMC modeling is whether the experimentally observed radiation occurs *only* from excited states of CO formed *on the surface* (surface mechanism). We

sought to investigate whether in fact the experimental data could be consistent with a two step mechanism where ground state CO formed on the surface from the first part of the O pulse was then vibrationally excited from O atoms from the 'tail' of the pulse (gas-phase mechanism). In other words we sought to distinguish between two different mechanisms to produce vibrationally excited CO:



or



The possibility of gas-phase CO excitation is suggested by the striking similarity between the observed gas-surface spectra and gas phase O + CO spectra from 4-6 μm , which both show a similar high degree of CO vibrational excitation.

Time History

Figure 2 shows experimentally observed time resolved intensities for 10 km/s atomic oxygen on graphite from Ref. 5 in a band pass from 4.5 to 5 μm (excited CO) along with the DSMC calculated CO one photon decay rates (photons/sec) as a function of time for a very narrow field of view ($\sim 1 \text{ cm}$ or "peak") and for a 50 cm \times 50 cm field of view, all normalized to their respective maxima. Time zero corresponds to the initiation of the O atom pulse flux at the source and the length in time of the pulse is indicated starting at the time when the head of the pulse first impacts the surface. The calculated "peak" time trace tracks the maximum for side-on (perpendicular to the beam) detector viewing. The 50 cm \times 50 cm result is for a side-on field of view centered on the surface, and is a reasonable guess of the actual field of view. These calculations assume that all CO excited states are formed by the "surface" mechanism. All curves reach their maxima as the tail of the O atom pulse hits the surface, which is physically reasonable. The decay of the curves with time is due mostly to excited CO leaving the field of view, which is most pronounced when following the "peak". The CO photon decay time for most of the CO vibrational states is long on this time-scale. The CO agreement between the calculated and 50 cm \times 50 cm field of view results and the experimental measurement suggests that the basic physics of the experiment is being reflected in the DSMC calculations.

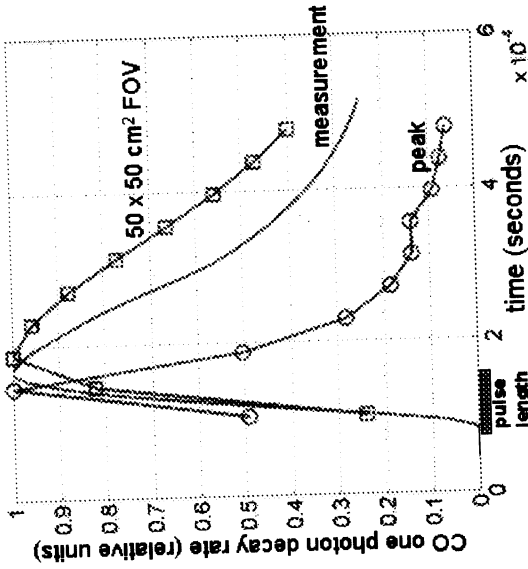


Figure 2. Measured (solid line), calculated peak (line with circles) and calculated 50 cm \times 50 cm field of view (line with squares) CO decay rates assuming a surface mechanism.

Figure 3 shows the same results for the surface mechanism for the 50 cm \times 50 cm field of view and the measurements, but in addition also shown is the photon decay rate assuming that excited CO is formed only by the gas-phase mechanism. The units are the total number of photon decays per second within the field of view and the measured results have been scaled an arbitrary amount to put them on the same scale. It is remarkable that the gas-phase curve follows the same basic time behavior as the surface measurement and also that it recovers about half of the intensity.

To understand the magnitude of these values we can estimate the photon decay rate by the surface mechanism as follows:

$$N_p \times p \times (1/\tau) = \text{CO surface mech. decay rate}, \quad (7)$$

where N_p is the number of oxygen atoms per pulse, p is the probability of producing a vibrationally excited CO state on the surface, and τ is the radiative lifetime. For the CO(v=1) contribution this is $3.7 \times 10^{-18} \times 0.0057 \times (1/0.033 \text{ sec.}) = 6.4 \times 10^{-17} \text{ sec.}^{-1}$, about one tenth of the total, the rest of the intensity coming from higher vibrational states. For the gas-phase mechanism we can make the following very rough approximation:

$$N_p \times [O] \times p \times 1 \times \sigma \times (1/\tau) = \text{gas-phase decay rate}, \quad (8)$$

sec^{-1} which again is about one tenth of the total for the gas-phase mechanism.

The experimental measurements did not spatially resolve the detected infrared radiation, but highly informative spatially resolved quantities may be generated from DSMC results. Figure 4 shows column densities for oxygen atom for a $100 \text{ cm} \times 100 \text{ cm}$ field of view from a side-on detector geometry. Each frame corresponds to a time snapshot every 4.2×10^{-5} seconds starting at 4.2×10^{-5} seconds. The oxygen atom source is actually outside this field of view and only part of the full pulse is seen in the first frame. At 10 km/s , the pulse moves $\sim 40 \text{ cm}$ from frame to frame before impacting the surface at frame three. At frame four, the entire pulse has hit the surface, and then slows down appreciably due to an assumption of full thermal accommodation of "unreacted" atomic oxygen. Some of the beam extends past the surface and therefore moves around it and this is visible as well. The computational grid stops just downstream of the surface and is indicated by the arrow in the last frame. Particles moving past here are removed from the simulation.

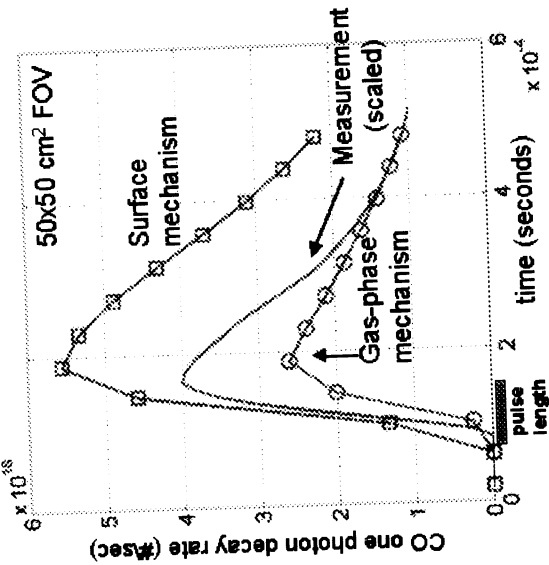


Figure 3. Calculated CO one photon decay rates for a $50 \text{ cm} \times 50 \text{ cm}$ field of view for surface and gas-phase mechanisms along with measurements (scaled).

where N_p is the number of oxygen atoms in the pulse, $[O]$ is the number density of O atoms from the pulse at the surface, p is probability of producing ground state CO from the surface, l is length scale of a region near the surface where most of the excited CO is formed and σ is the $O + CO(v=0) \rightarrow O + CO(v>0)$ excitation cross section. For producing $CO(v=1)$ this is approximately $3.7e18 \times 3.e13 \text{ cm}^{-3} \times CO(v=1)$ this is $0.08 \times 10 \text{ cm} \times 1.e-16 \text{ cm}^2 \times (1/0.033 \text{ sec}) = 2.7e17$

Figure 5 shows the column densities of the single photon decay rate from $CO(v=1)$ when viewed from a detector perpendicular to the O atom beam axis. These results assume the gas-phase only mechanism for producing excited state CO, but the direct surface mechanism results are nearly the same except they are about twice the magnitude. Each frame shows a step of 4.2×10^{-5} seconds in time starting at 2.1×10^{-5} seconds. These time-dependent quantities are averaged over the 4.2×10^{-5} second interval. In the first two frames, the O atoms have not yet reached the

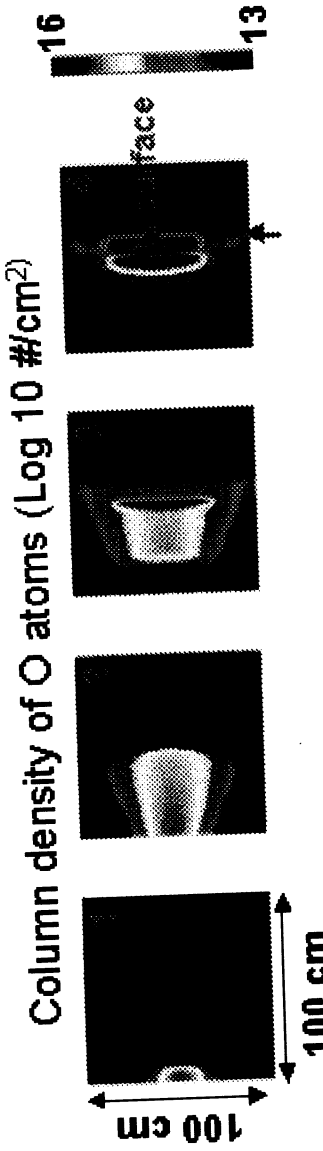


Figure 4. Column density of atomic oxygen pulse. Each time frame advances 4.2×10^{-5} seconds.

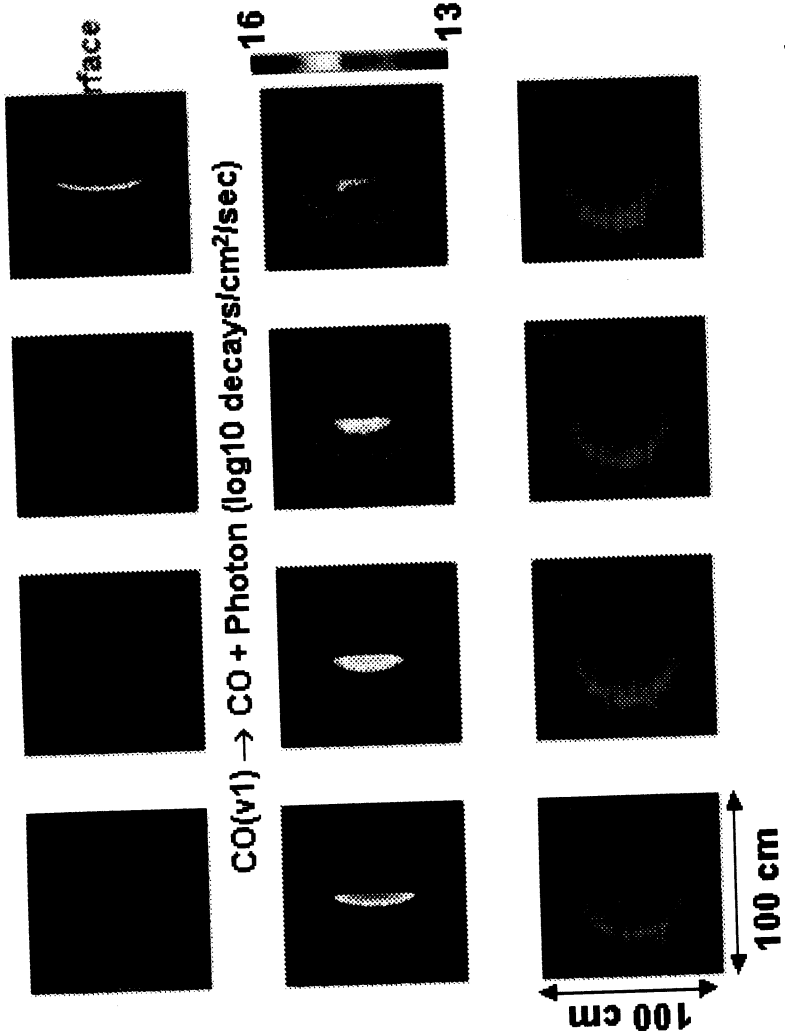


Figure 5. Time snapshots of the $\text{CO}(v_1)$ decay rate viewed from a side-on detector, assuming the gas-phase mechanism.

surface and no excited CO is yet formed. Photons from excited state decay become apparent in the third frame. Excited CO appears to be formed very near the surface. The radiation expands and diffuses with time as the excited CO moves out from where it was initially formed.

Figure 6 shows the reaction rate for formation of excited CO by the gas phase reaction, $\text{O} + \text{CO}(v=0) \rightarrow \text{O} + \text{CO}(v=1)$ for the gas-phase mechanism case. As expected the excited CO is formed near the surface, where the density of CO is likely to be highest. The timing of these frames is slightly shifted compared to the oxygen atom pulse densities shown earlier, and begin at 2.1×10^{-5} seconds (like the decay rate), so that the maximum of the $\text{CO}(v_1)$ formation rate corresponds to the tail end of the O atom pulse getting near the surface.

As a further confirmation step of the MBS calculations we computed the radiation maxima at 4 cm and 17 cm in front of the surface with a narrow field of view as a function of time. This was also done experimentally to estimate the excited state velocities leaving the surface. We obtained a value of 1.1 km/s for the simulation using the gas-phase

mechanism and 1.3 km/s for the simulation using the surface mechanism, compared with an experimental value of 1.3 km/s. These results indicate that, given the severe assumptions in modeling the chemical reactions, the experimental time signature results appear to be consistent with both the gas-phase and surface mechanisms for producing excited CO.

Spectral Analysis

The experimental data also include spectra taken at the peak time in spectral bands of $\sim 0.5 \mu\text{m}$ from 1.5 to $5.5 \mu\text{m}$. In Ref. 5, a spectral fit was performed which yielded assignments for CO, CO_2 and OH. A vibrational temperature of 10,000 K and a rotational temperature of 2,000 K were found for CO. The absolute intensity value was related to an overall efficiency for producing excited CO. The CO_2 was not fit explicitly but was assigned to fill in intensity through the presence of impurities.

Figure 7 shows the number densities of the DSMC calculated ground and excited vibrational states of CO in a $50 \text{ cm} \times 50 \text{ cm}$ field of view for the

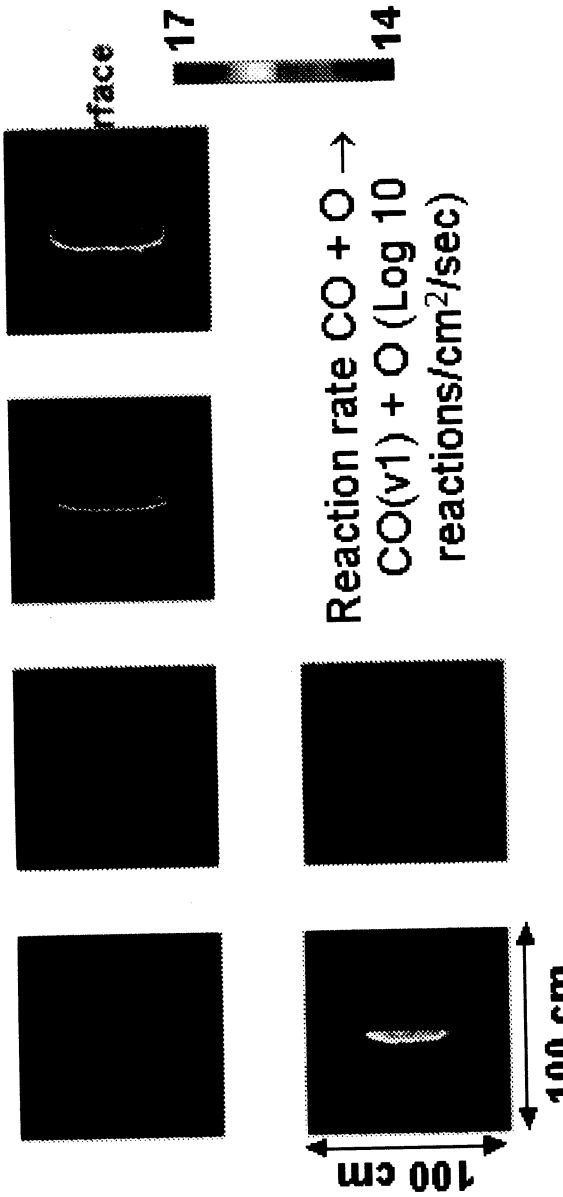


Figure 6. Time snapshots of the reaction rate for $O + CO \rightarrow O + CO(v_1)$ as a function of time when viewed side-on from the detector.

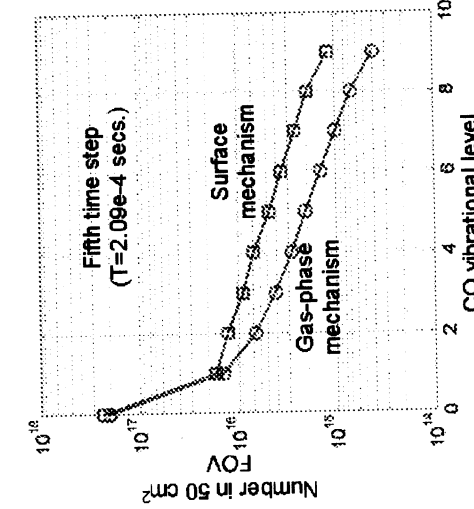


Figure 7. Calculation number of CO vibrational states in a 50 cm x 50 cm field of view for the surface and gas phase mechanisms.

surface and gas-phase mechanisms. These were from the fifth time step which is the peak in the radiation intensity and should reflect the observed spectral distribution. The surface mechanism yields excited CO which are a bit "hotter" than those in the gas-phase mechanism, but the distributions are in general quite close and should yield similar spectra.

Since we obtained the CO excited state formation probabilities for the surface mechanism DSMC calculations from the experimental spectral fits, the surface mechanism spectra are by definition

close to the experimental spectra. We now compare the gas-phase mechanism DSMC spectra with the experimental one. This is shown in Figure 8. To generate the spectra the DSMC number densities of $CO(v=0-9)$ have been converted to $W/sr/micron$ spectra assuming that the gas is optically thin and performing the radiation transport with data from the HTRAN data base.¹² These results were then normalized to the peak of the experimental spectra just below $5 \mu m$ and given $W/cm^2/sr/micron$ units by dividing by an assumed detector area $A=82 cm^2$. This area was not available from the experimental study⁵ and will be treated as an unknown in the present analysis. If we divide the original number densities by 10, which reflects the experimentally reported flux in the O atom pulse, the calculated area then certainly falls in a reasonable range. The absolute values of the number densities for the gas-phase (and surface) mechanisms for these DSMC calculations are therefore consistent with the experimentally observed ones. An assumed value of 2,000 K for the CO rotational temperature was used. Further work could refine this estimate based on the calculated DSMC $CO(v)$ internal energies. CO_2 spectra were generated with the FLAMES code¹³ with an assumed temperature of 700 K for rotation and vibration. These high resolution spectra ($5 cm^{-1}$) were then transformed into "bar spectra" by convolution with a $0.5 \mu m$ Gaussian filter and summed within the experimental pass-bands. There is generally good

agreement between the DSMC and experimental spectra, except between 2 and 3 μm . This is in the

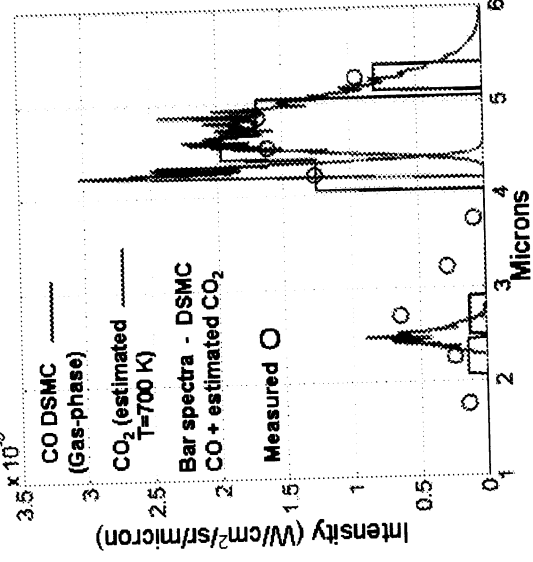


Figure 8. DSMC calculated and experimentally measured spectra.

region of the CO overtone band. This difference was assigned in the original experiment to OH, which we note could only be formed through an impurity in the measurement. However, we also note that it is possible that like CO, ground state CO₂ may be formed on the surface. Then through gas-phase excitation of CO₂, both CO and CO₂ might be formed.¹⁴



It may be that this extra CO makes up some of the difference in this overtone region between the DSMC calculations and the measurements. This will also change the spectral distribution from 4.5 μm . The chemistry of gas-phase O + CO₂ excitation is complex¹⁵ and its incorporation will be the subject of future work. Certainly higher resolution measured spectra would be extremely helpful in sorting out this chemistry.

Short Pulse Results

It may be possible to distinguish between the gas-phase and surface mechanisms through changing the duration of the O atom pulse in the experiment. If the pulse is short enough, the gas-phase mechanism should become less important compared to the surface mechanism which should be mostly independent of the pulse length. For short enough

pulses in the gas-phase mechanism, there will not be enough CO's formed near the surface to be excited by the tail of the pulse. To investigate this we performed an additional series of DSMC calculations for pulse lengths of 0.7e-5, 2.8e-5, and 4.9e-5 seconds. All other parameters in the DSMC calculation remained the same. We defined a conversion efficiency:

$$\text{Efficiency} = (\text{decays/sec}) / (\text{Np} \times \text{p} \times (1/\tau)), \quad (10)$$

where decays/sec is the total number of v=1 to v=0 decays/sec in a 50 cm x 50 cm field of view, Np is the number of O atoms in the pulse, p is the probability of forming ground state CO(v=0), and τ is the v=1 to v=0 decay time. For the surface mechanism, the efficiency should be close to 1.0 and should be independent of pulse length. Figure 9 shows the results of these parametric calculations. As expected the gas-phase mechanism efficiency is a strong function of the pulse duration time, and suggests possible future experiments to distinguish the two mechanisms.

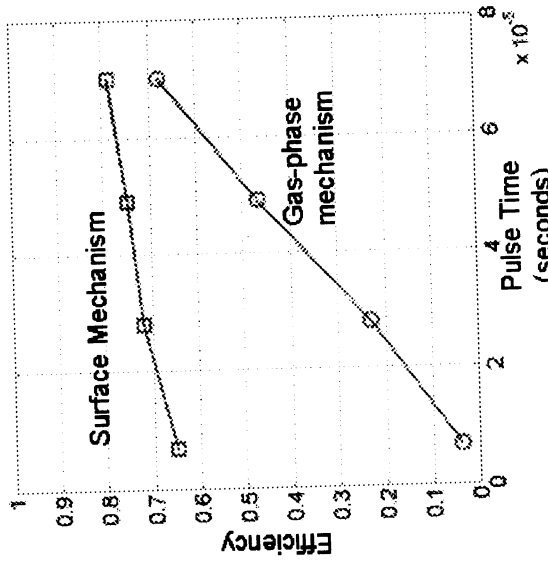


Figure 9. Calculated efficiencies of producing radiation from CO(v1) as a function of pulse duration time.

Density Effects

As noted before, the source parameters used in these calculations lead to a flux which is about 10⁵ times that reported in the experimental description. We have rerun our DSMC calculations with a source number density (and therefore O atom flux) which is 10 times less. For the surface mechanism the amount

of radiation produced should be a straight scaling of the higher flux results, but for the gas-phase mechanism we find that the smaller flux results are about six times smaller than direct scaling predicts. The radiation time trace is quite similar, however. The gas-phase mechanism depends on the build-up of CO near the surface, and this is a complex function of the time of the pulse and its density. We note, however, that the smaller source flux gas-phase radiation intensity levels are still within the unknown modeling parameters of the experiment. Future work will explore further these density effects.

Summary

With a new DSMC code called the Molecular Beam Simulator (MBS), we have performed time-dependent (unsteady) calculations to model a pulsed gas-surface experiment where 10 km/s oxygen atoms impact graphite. Experimental data consisted of radiant intensity time traces and molecular spectra from 1.5 μm to 5.5 μm of excited state species, mainly CO, observed near the surface. The MBS calculations suggest that two different mechanisms for forming molecular excited states are *both* consistent with the experimental data. In the first mechanism excited CO is formed directly on the surface, and in the second ground state CO formed on the surface is later vibrationally excited in the gas-phase by the tail of the O atom pulse. The calculations also show that experiments with shorter pulse lengths will greatly lessen the latter, gas-phase mechanism efficiency in producing excited molecular states, but should not greatly affect the direct surface mechanism. High resolution spectra are generated from the calculations as well, and indicate the rich information that could be obtained from such a measurement.

There are many approximations used in the in the DSMC calculations. The simplified chemistry of product formation on the surface and the assumption of isotropic scattering of products in gas phase scattering are among the many severe approximations in the modeling. Nevertheless, the present study shows that the MBS code can capture the basic features of the experimental observables and therefore can be a valuable analysis tool. The MBS code can also be used as an aid in designing experiments by simulating them before-hand. These simulations could suggest optimal important experimental design parameters, like sensor placement, source fluxes, surface target placement, etc. Furthermore, it may be possible to use the MBS

code to examine more stressing experimental conditions, such as higher source densities and background pressures. These experimental conditions are normally difficult to analyze, but should be amenable to modeling with the present DSMC approach which explicitly includes multiple collision events.

Acknowledgments

This work was funded through a NASA Phase II Small Business Innovative Research (SBIR) award, C NAS8-00201. Grateful acknowledgment is made to A. Finchum at NASA Marshall Space Flight Center for technical monitoring and guidance.

References

1. Bird, G. A. "Molecular Gas Dynamics and the Direct Simulation of Gas Flows", Clarendon Press, Oxford, (1994).
2. Harvey, J. K. and Gallis, M. A. "Review of Code Validation Studies in High Speed Low-Density Flows", J. Spacecraft and Rockets, Vol. 37, pp. 8-20. (2000).
3. Braunstein M. and Wysong I. J., "Direct Simulation Monte Carlo Modeling of High Energy Chemistry in Molecular Beams: Chemistry Models and Flowfield Effects", 22nd International Rare Gas Dynamics Conference, Sydney Australia, July, 2000.
4. Cho, J., Braunstein, M., and Elgin, J., "SOCRATES3.0 Users' Manual", Air Force Research Laboratory technical Report, AFRL-VS-TR-1999-1535, (June, 1999).
5. Holtzclaw K. W., Fraser, M. E., and Gelb, A., "Infrared Emission From the Reaction of High Velocity Atomic Oxygen with Graphite and Polyethylene", J. Geo. Research 95, 4147-4153 (1990).
6. Minton T. K. and Garton D. J., "Dynamics of Atomic-Oxygen-Induced Polymer Degradation in Low Earth Orbit", in Chemical Dynamics in Extreme Environments: Advanced Series in Physical Chemistry, ed. R. A. Dressler (World Scientific, Singapore, (2000).
7. Leger, L. J. and Visentine J. T., "A Consideration of Atomic Oxygen Interactions with the Space Station", J. Spacecraft, vol. 23, pp.505-511 (1986).
8. Cohen, L. K., "A Lower Bound on the Loss of Graphite by Atomic Oxygen Attack at Asymptotic Energy", J. Chem. Phys. pp. 9652-9663.

9. UPSCHULTE, B. L. and CALEDONIA G. E., "Laboratory Measurements of Infrared Excitation Cross Sections of Fast O-atom Collisions with CO, CO₂, and CH₄", *J. Chem. Phys.*, **96**, pp. 2025-2033 (1992).
10. BROOK, J. W., "Far-field Approximation For a Nozzle Exhausting Into a Vacuum", *J. Spacecraft and Rockets*, **6**, 626 (1969).
11. BRAUNSTEIN M. and DUFF J., "Electronic Structure and Dynamics of O + CO Collisions", *J. Chem. Phys.*, **112**, 2736-2745 (2000).
12. ROTHMAN L. S., GAMACHE R. R., GOLDMAN A., BROWN L. R., TOTH R. A., H. M. PICKETT, POYNTER R. L., FLAND J. M., CAMY-PETYET C., BARBE A., HUSSON N., RINSLAND C. P., and SMITH M. A. H., "The HITRAN Molecular Database: Editions of 1991-1992", *J. Quant. Spectrosc. Radiat. Transfer*, Vol. **48**, p. 469 (1992).
13. BERNSTEIN, L. S., SUNDBERG, R. L., ZAKIN, M. R., SELBY, J. E., FREEMAN, G. N., and CROW, D. R., "Nonequilibrium High Altitude Rocket Plume Signature Model", 1990 Meeting of the Infrared Information Symposia Specialty Group on Targets, Backgrounds and Discrimination, Vol. 1 213400-37-X(1), March 1990, pp. 47-68.
14. CALEDONIA, J. B. "Infrared Radiation Produced in Ambient/Spacecraft-Emitted Gas Interactions Under LEO Conditions", AIAA 00-0104, 38th AIAA Aerospace Sciences Meeting and Exhibit, 10-13 January 2000, Reno, Nevada.
15. SCHATZ, G. C., and REDMON, M. J. "A Quasiclassical Trajectory Study of Collisional Excitation in O(³P) + CO₂", *Chem. Phys.*, **58**, pp. 195-201 (1981).